Measurement of Dynamic Joint Stiffness from Multiple Short Data Segments

Kian Jalaleddini, *Member, IEEE*, Mahsa A. Golkar, *Student Member, IEEE*, and Robert E. Kearney, *Fellow, IEEE*

***Abstract*— This paper presents our new method, *Short Segment-Structural Decomposition SubSpace* (SS-SDSS), for the estimation of dynamic joint stiffness from short data segments. The main application is for data sets that are only piecewise stationary. Our approach is to: 1) derive a data-driven, mathematical model for dynamic stiffness for short data segments; 2) bin the non-stationary data into a number of short, stationary data segments; and 3) estimate the model parameters from subsets of segments with the same properties. This method extends our previous state-space work by recognizing that initial conditions have important effects for short data segments; consequently, initial conditions are incorporated into the stiffness model and estimated for each segment. A simulation study that faithfully replicated experimental conditions delineated the range of experimental conditions for which the method can successfully identify stiffness. An experimental study on the ankle of a healthy subject during a torque matching tasks demonstrated the successful estimation of dynamic stiffness in a slow, time-varying experiment. Together, the simulation and experimental studies demonstrate that the SS-SDSS method is a valuable tool to measure stiffness in functionally important tasks.**

***Index Terms*— Biological system modeling, biomechanics, biomedical signal processing, nonlinear dynamical systems, state-space methods, system identification.**

I. Introduction

DYNAMIC joint stiffness, also referred to as impedance [1], [2] or its inverse admittance [3], describes the dynamic relation between the position of a joint and the torque acting about it [4]. Joint stiffness plays a critical role in the control of posture and locomotion [5]–[8]. Thus, constructing mathematical models that accurately describe these dynamics is important to understand the control of functional tasks. Such mathematical models give insight into how the underlying neuromuscular mechanisms interact together to perform a task. They provide objective measures for diagnosis, assessment, and treatment monitoring of the neuromuscular diseases that change muscle tone. Furthermore, they can provide the normative information needed for the design of rehabilitation devices intended to normalize the mechanical properties of an artificial or impaired joints [9]–[13].

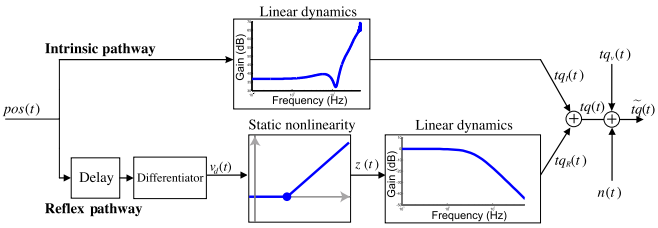

Fig. 1. Parallel-cascade structure of ankle joint stiffness. The input is joint angular position and the output is total joint torque, the sum of the intrinsic, reflex and voluntary torques and measurement noise. The intrinsic pathway acts as a high-pass filter and the reflex pathway has a block-oriented, nonlinear model. Adapted from [14].

Dynamic stiffness can be described with a *parallel-cascade* (PC) model consisting of two parallel pathways (Fig. 1): (i) intrinsic stiffness which models visco-elastic and inertial properties of the joint, active muscles, and passive tissues; it has high-pass filter dynamics, (ii) reflex stiffness arising from changes in muscle activation due to stretch reflex mechanisms; it has a block-oriented, nonlinear structure comprising a differentiator cascaded with a delay, a static nonlinearity resembling a rectifier, and a linear, low-pass filter [4].

The PC model successfully describes the dynamic relationship between the position and torque at the ankle and a variety of other joints for stationary conditions [4], [12], [15]–[18]. However, the stationarity assumption is often violated during functionally important tasks when the joint operating point is not fixed. Examples include locomotion when the muscle active state and/or length undergo large changes [1], [19]–[22], upright stance where the control strategy may change with postural sway [23], and high force contractions which may result in muscle fatigue [24].

Marmarelis et al. proposed that for linear systems, the non-stationarity issue could be addressed by segmenting non-stationary data records into short, stationary data segments and then constructing local, linear, time-invariant models from subsets of segments with the same properties [25]. A similar approach to the measurement of joint stiffness would have important applications. For instance, when stiffness dynamics

Manuscript received June 1, 2016; revised December 1, 2016; accepted January 16, 2017. Date of publication March 2, 2017; date of current version August 6, 2017. This work was supported in part by the Canadian Institutes of Health Research, in part by the Fonds Québécois de la Recherche sur la Nature et les Technologies, and in part by the Natural Sciences and Engineering Research Council of Canada.

K. Jalaleddini is with the Division of Biokinesiology and Physical Therapy, University of Southern California, Los Angeles, CA 90033 USA (e-mail: seyed.jalaleddini@mail.mcgill.ca).

M. A. Golkar and R. E. Kearney are with the Department of Biomedical Engineering, McGill University, Montréal, QC H3A 2B4, Canada (e-mail: mahsa.aliakbargolkar@mail.mcgill.ca; robert.kearney@mcgill.ca).

Digital Object Identifier 10.1109/TNSRE.2017.2659749

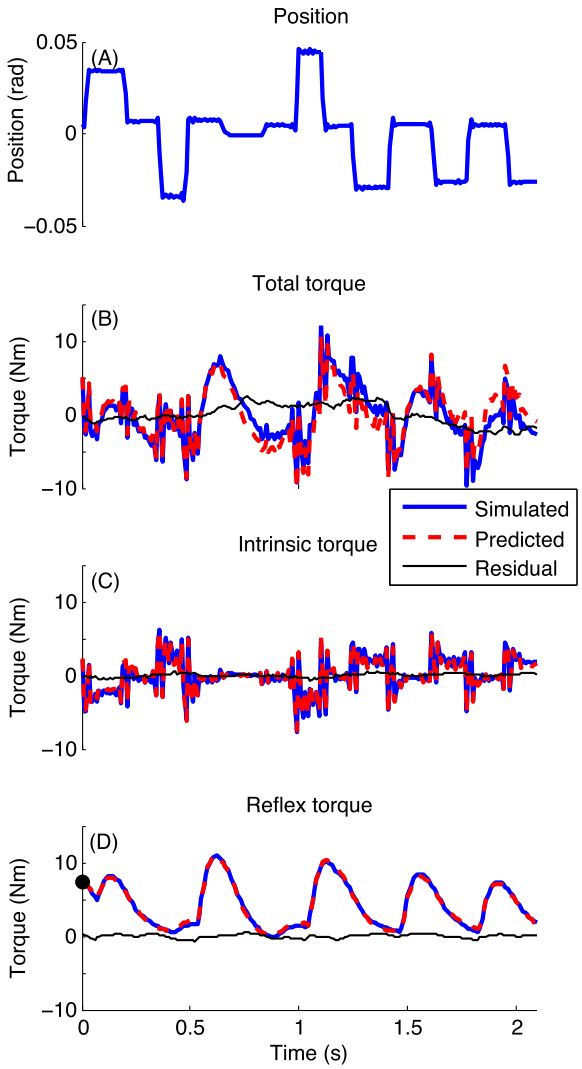

Fig. 2. A segment from a typical Monte-Carlo run with 20 segments with SegLen = 2s, SNR = 10dB, and RtI = 3. (A) position; (B) total torque; (C) intrinsic torque; (D) reflex torque. Each torque panel shows the noise-free simulated and predicted torques and their residuals (difference).

vary slowly with time during quiet stance, one could segment the data to estimate models describing the different strategies used for balance control. Segmentation would also be useful in estimating stiffness at high activation levels where it is difficult to maintain stationary contractions for extended periods. Consequently, it would be very valuable to have a method to estimate stiffness from short, stationary data segments and this paper presents the *Short Segment - Structural Decomposition, SubSpace* (SS-SDSS) method that meets this need.

II. Mathematical Model and Method

This section presents an overview of the novel SS-SDSS method for measurement of stiffness from short data segments. A detailed derivation of the method is available as supplementary material. The code has been released in our *NonLinear Identification* (NLID) toolbox with a number of examples and demos available for download from our public GitHub repository (reklab_public).[1]

[1]https://github.com/reklab/reklab_public

Fig. 1 shows the PC structure of ankle joint stiffness. The intrinsic pathway represents the mechanical properties of the joint and is modelled as a linear, short, two-sided *Impulse Response Function* (IRF) with unknown coefficients, whose length is less than the reflex delay [26]. This IRF will have high-pass dynamics due to the viscous and inertial properties of the intrinsic pathway.

The reflex pathway model has a time-delay due to the delay in propagation of action potentials to and from the spinal cord. It also comprises a differentiator, followed by a static nonlinearity, and a linear dynamic block. The differentiator represents the rate sensitivity of reflex response that prevails when the variation in joint angular position is small [3]. The static nonlinearity represents the asymmetric spinal reflexes that are larger for the ankle plantarflexor than dorsiflexor muscles. Such an asymmetric, rate sensitive reflex response has been reported in both lower and upper extremities [27], [28]. The static nonlinearity is approximated by a basis function expansion of the delayed velocity using Tchebychev polynomials. The linear dynamics, which represent the dynamics of the sensory receptors and muscle's activation-contraction dynamics [29] are modelled with a linear, state-space model.

Combining the intrinsic and reflex models gives a linear, *Multiple-Input-Single-Output* (MISO) state-space model that approximates the *Single-Input-Single-Output* (SISO), nonlinear PC structure. The MISO model for the i-th segment is [14]:

$$\begin{cases} \mathbf{X}^i(k+1) = A_R\mathbf{X}^i(k) + B_T\mathbf{U}_T^i(k) \\ \tilde{tq}^i(k) = C_R\mathbf{X}^i(k) + D_T\mathbf{U}_T^i(k) + e^i(k) \end{cases} \tag{1}$$

where $\tilde{tq}^i(k)$ is the measured total torque, $\mathbf{U}(k)$ is the constructed input consisting of lagged values of position and Tchebychev basis expansion of delayed velocity (see supplementary materials for details), $\mathbf{X}(k)$ contains the system states, and $e^i(k)$ is the output noise. A_R and C_R are the state-space matrices of the reflex linear dynamics. The elements of the B_T and D_T matrices are functions of the coefficients of the intrinsic IRF, the coefficients of the reflex nonlinearity's basis expansion, and the state-space matrices of the reflex linear dynamics (see supplementary materials).

Expanding (1) gives the key data equation:

$$\begin{aligned} \tilde{tq}^i(k) = C_R A_R^k \mathbf{X}^i(0) + \sum_{r=0}^{k-1} C_R A_R^{k-1-r} B_T \mathbf{U}_T^i(r) \\ + D_T\mathbf{U}_T^i(k) + e^i(k) \end{aligned} \tag{2}$$

which shows that the total measured torque is a function of the past and current inputs as well as the segment's *Initial Conditions* (IC). Note that it is common practice in constructing mathematical models for biological systems to ignore the transient responses $C_R A_R^k \mathbf{X}^i(0)$. This is reasonable when the data length is much greater than the transient response because $\lim_{k\to\infty} A_R^k = 0$ for stable systems. However, for short segments, where the length of each data segment may be comparable to that of the transient response, the contribution of the IC to the output must be included in the data equation to avoid biasing the estimates [30].

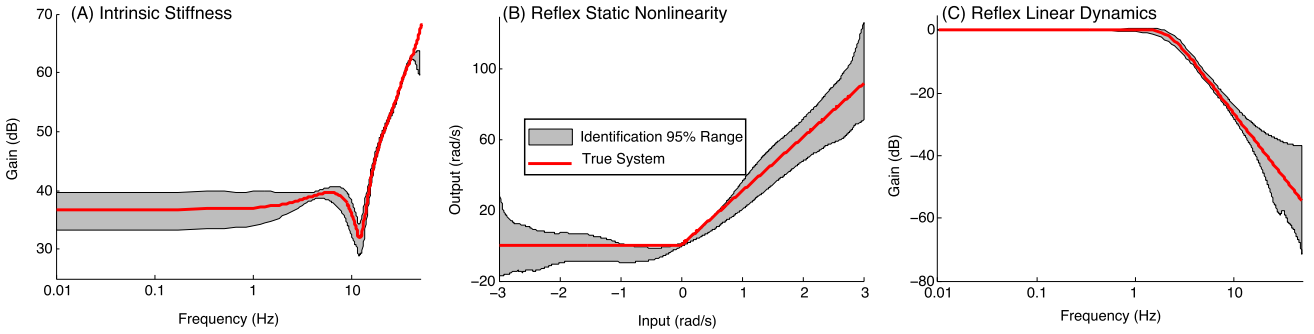

Fig. 3. Typical Monte-Carlo identification ranges from the simulation study with 200 trials where stiffness was estimated with NumSeg = 20, SegLen = 2s, SNR = 10dB, and RtI = 3: (A) gain of the intrinsic stiffness frequency response function; (B) reflex static nonlinear element; (C) gain of the linear dynamics of the reflex stiffness frequency response function.

The new SS-SDSS method estimates the parameters of this model from multiple short segments by using and extending several techniques:

- The Hankel matrices in the *Multivariable Output Error SubsPace* (MOESP) data equation of [31] are extended to support multiple, arbitrary-length segments. The A_R and C_R state-space matrices are then extracted using a method based on MOESP [31].
- The decomposition step of SDSS is used to decompose the intrinsic and reflex torques [14].
- The *New SubSpace* (NSS) Hammerstein identification method of [32] is extended to estimate the ICs of each segment as well as the parameters of the static nonlinearity and linear dynamics of the reflex stiffness pathway from the position-reflex torque data. This is achieved by augmenting one of the regressors of the NSS with the transient response $C_R A_R^k$ to estimate the ICs. The supplementary materials provide a detailed description of the model formulation and the method.

III. Simulation Studies

A. Simulation Methods

1) Simulation Models: The model of the PC structure of stiffness, shown in Fig. 1, was simulated using MATLAB. The parameter values were based on those reported for subjects executing tonic isometric contractions of the calf muscles [33]. The intrinsic pathway model was IRF representation of the frequency response function shown in Fig. 3(A); this was estimated from experimental data and had high-pass dynamics. For the reflex pathway: the delay was set to 40ms; the static nonlinearity was modelled as a half-wave rectifier; and the linear element modelled as the low-pass filter [33]:

$$\frac{184.96}{s^2 + 16.8s + 184.96} \tag{3}$$

Fig. 3(B) and (C) visualize these components. Simulations were done at 1kHz and signals were decimated to 100 Hz for analysis.

2) Input and Noise Signals: The performance of any identification algorithm will depend strongly on the frequency content and amplitude distribution of the input and noise signals [34]. These will be particularly important in stiffness experiments because the low-pass, nonlinear dynamics

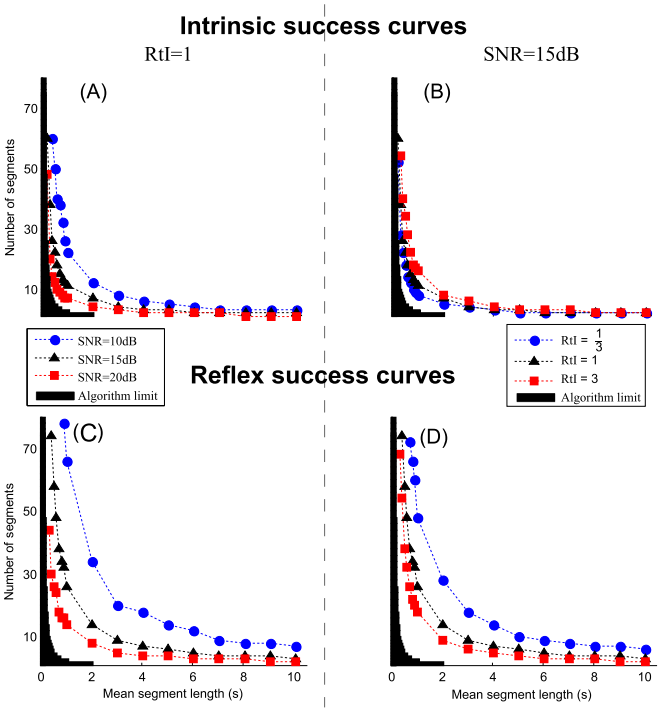

Fig. 4. Success curves for the identification of the intrinsic and reflex pathways. Each point indicates the minimum number of segments required at a mean segment length for successful identification. (A,B) success curve for the identification of intrinsic pathway: (A) changes with SNR when RtI = 1 (simulation only); (B) changes with RtI when SNR = 15 (dB) (simulation and experiment); (C,D) success curve for the identification of reflex pathway: (C) changes with SNR when RtI = 1 (simulation only); (D) changes with RtI when SNR = 15dB (simulation and experiment). The black area shows the algorithm theoretical limits where the algorithm does not work.

of the actuator applying perturbations and the actuator-joint fixation make it almost impossible to apply an ideal input. Furthermore, the inevitable fluctuation of torque in tonic, isometric contractions results in a complex noise [35], [36]. Consequently, as in our previous work [14], the position input and noise sequences were drawn from a library of 210 experimental records to ensure that the simulations were as realistic as possible. Thus, the library position records were acquired when *Pseudo Random Arbitrary Level Distributed Sequence* (PRALDS) inputs were applied to hydraulic actuator. Noise records were measured as subjects maintained tonic,

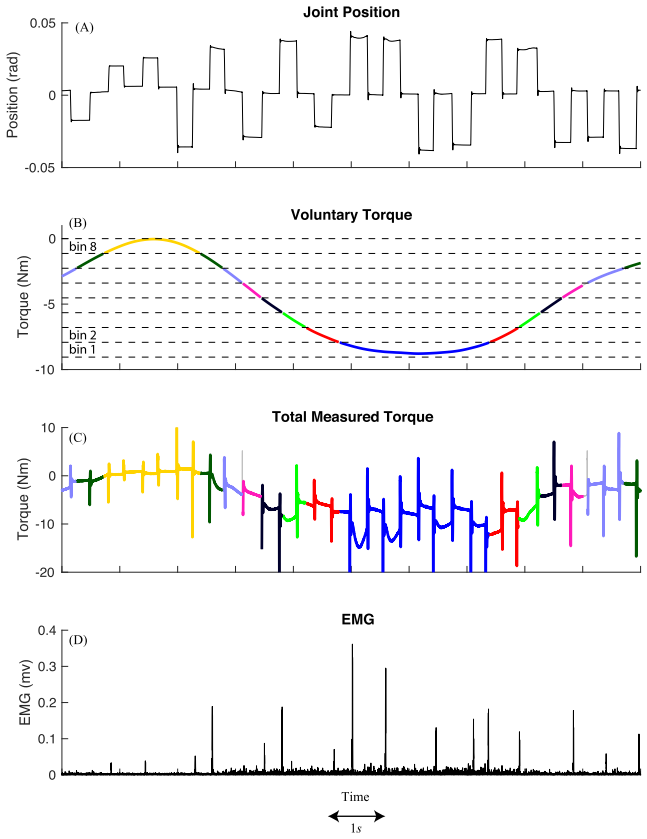

Fig. 5. Representative data and the binning technique in a torque matching experiment: (A) position perturbations signal; (B) estimated voluntary component of the torque. The voluntary torque was used to bin the non-stationary data into 8 bins; (C) total measured torque that; (D) EMG.

isometric contraction with no position perturbation (see supplementary materials).

Factors studied: We evaluated how the performance of the algorithm depended on four factors important in practice. These included system factors:

(i) The overall *Signal to Noise Ratios* (SNR) defined as:

$$\text{SNR}_{\text{dB}} = 10log\frac{\text{power}(tq(k))}{\text{power}(e(k))} \tag{4}$$

SNRs of 10, 15 and 20dB were used as these span the range observed in our laboratory.

(ii) The ratio of *Reflex to Intrinsic* (RtI) torque power:

$$\text{RtI} = \frac{\text{power}(tq_R(k))}{\text{power}(tq_I(k))} \tag{5}$$

The relative power of the intrinsic and reflex torques influences the decomposition algorithm [14]. Experiments were done at RtIs of $\frac{1}{3}$, 1 and 3 corresponding to levels observed in normal subjects [33].

as well as data factors:

(iii) *Segment Lengths* (SegLen): Data were divided into segments whose lengths were drawn from a uniform random distribution. The minimum of the distribution was varied in the set $\{0.2, 0.3, \cdots, 1, 2, \cdots, 10\}$ (s) and the maximum was the minimum plus 100 ms.

(iv) *Number of Segments* (NumSeg): For each combination of SNR, RtI, and SegLen, we determined the minimum value of NumSeg required for *successful* identification.

Accuracy: We performed *Monte-Carlo* (MC) experiments. An MC series was deemed successful if the validation %VAF was greater than 95% in at least 95% of the trials:

$$\%\text{VAF} = 100\left(1 - \frac{\text{var}(\hat{y}(k) - y(k))}{\text{var}(y(k))}\right) \tag{6}$$

where $y(k)$ is the simulated noise-free output and $\hat{y}(k)$ is the output predicted by the estimated model. %VAFs were computed for intrinsic and reflex torques.

3) Monte-Carlo Analysis: The performance of the algorithm was evaluated by determining the minimum number of segments required for a successful identification-validation in a series of MC experiments.

Each MC series tested a combination of factors and had 200 trials. Each trial comprised an identification run followed by a validation run. For the identification run, we randomly selected realizations of the input and noise signals, simulated the system according to system factors, segmented the data according to data factors and identified the model with SS-SDSS. In the validation stage, We compared the predicted output of the model to the noise-free output of the true system when they both received a realization of input that was not used in the identification stage.

B. Simulation Results

Fig. 2 shows a segment from an identification run of a typical successful MC series. Three important points are evident. First, Fig. 2(B) shows that the predicted and measured total torques were very similar, indicating that the estimated model predicted the overall mechanical behaviour very well. %VAF was 99.6% for the intrinsic torque and 97.8% for the reflex torque. Second, the intrinsic (Fig. 2(C)) and reflex torques (Fig. 2(D)) were predicted accurately with very small residuals; this demonstrates that the decomposition was accurate. Third, the torque predictions were accurate at the start of each segment, indicating that the initial conditions were correctly estimated.

Fig. 3 shows the 95% confidence interval of the components of the parallel-cascade structure estimated for this MC series. These represent the range between 2.5 to 97.5 percentiles over the 200 identified models. It demonstrates that the estimated models were always close to the true system, the variability was low bracketed the true dynamics symmetrically indicating that the bias error was low.

Fig. 4 summarizes the performance of the algorithm as functions of the system and data factors in terms of success curves. Each point on the success curve corresponds to the minimum number of segments needed to ensure successful identification for the corresponding segment length.

The success curves for the intrinsic pathway as a function of SNR (Fig. 4(A)) and RtI (Fig. 4(B)) reveal three important points: (i) they resemble rectangular hyperbolas with the coordinate axes as their asymptotes; the shorter the SegLen, the higher the NumSeg required for a successful identification;

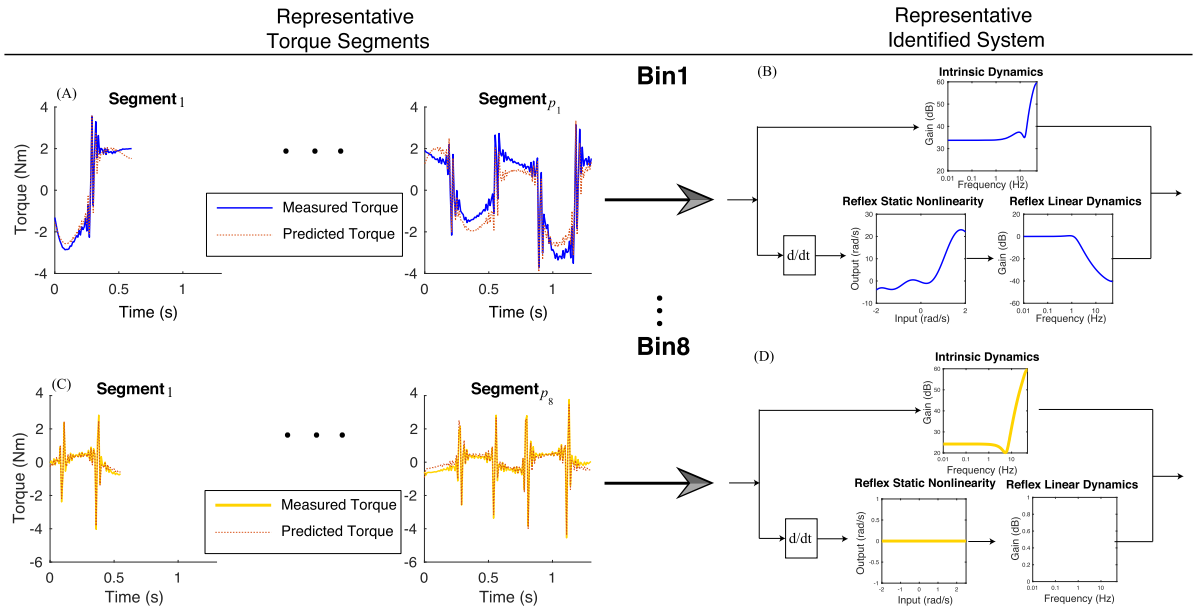

Fig. 6. Representative identified systems in a torque matching experiment: (A) typical measured torque segments from bin 1 and SS-SDSS predictions; (B) typical identified parallel-cascade structure for bin 1; (C) typical measured torque segments from bin 8 and SS-SDSS predictions; (D) typical identified parallel-cascade structure for bin 8.

(ii) the total number of samples required for a successful identification (mean SegLen $\times$ NumSeg) increases as the SNR level drops; (iii) the number of samples required for a successful identification was smaller for low values of RtI reflecting the lower relative size of reflex torques.

Success curves for identification of the reflex pathway as functions of the SNR (Fig. 4(C)) and RtI (Fig. 4(D)) were generally similar to those of the intrinsic pathway. However, two main differences are apparent. First, the reflex pathway always required more segments than the intrinsic pathway for a successful identification. Second, the number of samples needed to identify the reflex pathway decreased with RtI, reflecting the increased relative size of reflex torques.

IV. Application to Identification of Slowly Varying Stiffness

This section describes simulation and experimental studies demonstrating the application of the method when stiffness changes slowly with time.

A. Methods

1) Experimental Methods: A healthy female subject was recruited who gave informed consent to the experimental procedures, which had been reviewed and approved by McGill University Institutional Review Board. The subject lay supine with the left foot attached to a hydraulic actuator using a custom-made, low-inertia boot. The knee was immobilized in a fully extended position with straps and sandbags. The actuator was operated as a very stiff position-servo that controlled the angular position of the ankle. The neutral position (90 degrees angle between shank and foot) was taken as 0 rad; positions dorsiflexed from the neutral and torques tending to dorsiflex the ankle were taken as positive.

The mean joint position was placed at 0.2 rad. The joint was perturbed using realizations of PRALDS input with a maximum amplitude of 0.04 rad and switching times ranging from 250 and 350 ms. The subject generated a time-varying muscle contraction by tracking a visual target displayed on an overhead monitor aided by visual feedback of their low-pass filtered (8-th order Bessel filter with 0.7 Hz cut-off frequency) ankle torque. The target signal was a 0.1 Hz sinusoid with amplitude spanning 0 to 20% of plantarflexion *Maximum Voluntary Contraction* (MVC) torque. Five trials, each lasting 120 seconds were recorded. One minute of rest was imposed between trials to avoid fatigue.

The angular joint position was measured using a precision potentiometer (Model 6273, BI technologies) and joint torque with a 2110-5K, Lebow transducer. EMG signals were measured from the medial and lateral heads of the Gastrocnemius using single differential surface electrodes supplied with the Bagnoli systems. A DermaSport reference electrode was a placed on the kneecap which was immobilized throughout the experiment. EMG signals were amplified with a gain of 1000, bandpass filtered (20-2000Hz), sampled and full-wave rectified.

All signals were low-pass filtered at 486.3 Hz and digitized at 1 kHz with 24bits resolution using a set of NI-4472 A/D cards. Samples were decimated to 100 Hz prior to analysis.

2) Simulation Methods: The simulation study replicated the experimental conditions. Thus, the joint voluntary torque ($tq_v(k)$ in Fig. 1) was a 0.1 Hz sine wave whose amplitude ranged from 0 to 10 Nm. The intrinsic stiffness elastic parameter and reflex stiffness gain were varied with voluntary torque as shown in Fig. 8 based on the values reported in quasi-stationary experiments [33].

This time-varying model was simulated for 600 s. Input and noise sequences were randomly selected from the experimental

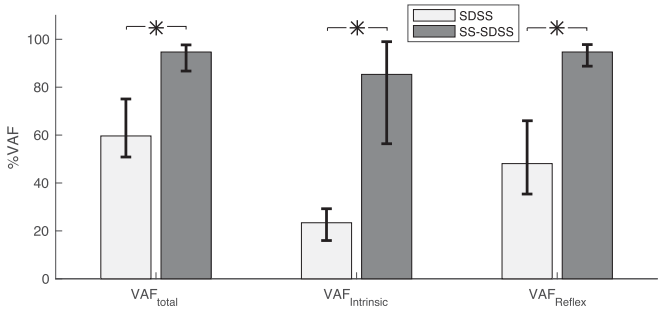

Fig. 7. Intrinsic and reflex identification %VAF (average bracketed by its 90% range) using the SDSS and SS-SDSS methods in the simulation study.

libraries described in Section III-A.2. Noise was added to the measured torque to give an effective SNR of 15 dB.

3) Data Preparation: The voluntary torque was estimated by low-pass filtering the measured torque using a two-sided, *Finite Impulse Response* (FIR) low-pass filter with break frequency of 0.2 Hz. Fig. 5 shows one period of a representative experimental trial. It is evident that the torque response (Fig. 5(C)) to the position perturbations (Fig. 5(A)) was non-stationary. Thus, the reflex EMG (Fig. 5(D)) and torque responses increased as the voluntary torque (Fig. 5(B)) became more negative.

For analysis, pools of quasi-stationary segments were assembled by binning the data according to the voluntary torque level. We used 8 equally distanced bins covering 5% to 95% range of the voluntary torque, as demonstrated in Fig. 5.

4) Identification: A boot-strap experiment consisting of 200 trials was performed to quantify the variance of the estimates. For each trial, segments were randomly drawn from each bin until 45000 total number of samples were collected from each bin.

SS-SDSS was applied to the selected segments of each trial of each bin (Fig. 6). SDSS was also applied to the concatenated segments. The main difference between SDSS and SS-SDSS is in identification of the ICs. For the simulation, differences between SDSS and SS-SDSS were quantified in terms of %VAF for intrinsic and reflex torques. For the experimental studies, where the true vales of the intrinsic and reflex torque are unknown, we used %VAF for total torque only. The significance of differences between %VAFs of the two methods was assessed with a sign test at a 5% significance level.

The accuracy with which each method recovered the intrinsic stiffness elastic parameter and gain of the reflex stiffness was assessed. Since these parameters are not available directly from SS-SDSS they were estimates as follows: the elastic parameter corresponds to the DC gain of the intrinsic stiffness dynamics and was estimated as the integral of the intrinsic stiffness IRF. The gain of the reflex pathway was estimated by first forcing the linear element to have unity gain so that all gain was associated with the static nonlinear element. The reflex gain was then estimated by using the trust-region reflective algorithm from MATLAB curve fitting

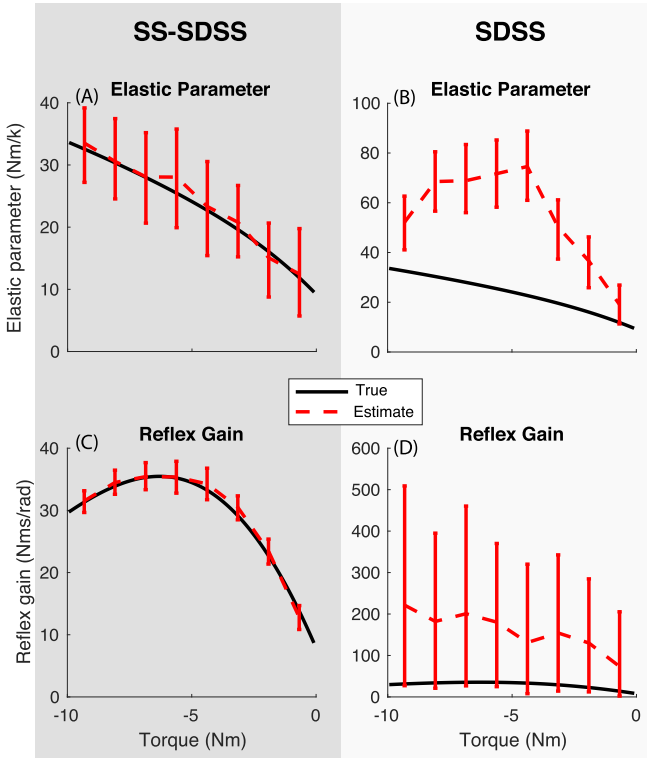

Fig. 8. Estimated (average bracketed by its 90% range) and true values of the intrinsic elastic parameter and reflex gain using the SS-SDSS (A,C) and SS-SDSS (B,D) methods in the simulation study.

toolbox to fit a threshold-slope model to the estimated static nonlinearity [14].

B. Results

1) Simulation Results: Fig. 7 demonstrates the identification %VAF for the intrinsic and reflex torques pooled from all the bins. It is clear that the %VAF resulted from the predictions of SS-SDSS estimates was always significantly larger than that from SDSS.

Fig. 8(A) shows the estimates of the intrinsic elastic parameter and the reflex gain as a function of joint torque. In general, both the intrinsic and reflex estimators captured the overall pattern of parameter modulation and provided unbiased estimates that symmetrically bracketed the true values. The variance of the elastic parameter was larger than that of the reflex gain. Fig. 8(B) shows the corresponding SDSS parameter estimates. They were biased and had large variance. Thus, the intrinsic parameter and reflex gain were both overestimated when SDSS was applied.

2) Experimental Results: Fig. 9 shows the total identification %VAF of the SDSS and SS-SDSS methods. For SS-SDSS, the mean %VAF was 87% demonstrating accurate identification. In contrast the mean %VAF was only 63% for SDSS demonstrating that it predicted the response much less accurately. Fig. 10 demonstrates the intrinsic stiffness elastic parameter and the reflex gain as a function of the voluntary torque. On average, they both increased with increase in the plantarflexing voluntary torque.

The results show a successful application of the SS-SDSS method in identifying stiffness from analyzing

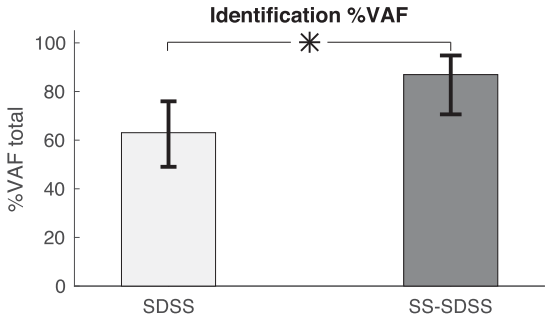

Fig. 9. Mean identification %VAF of total torque bracketed by its 90% range using the SDSS and SS-SDSS methods in the experimental study.

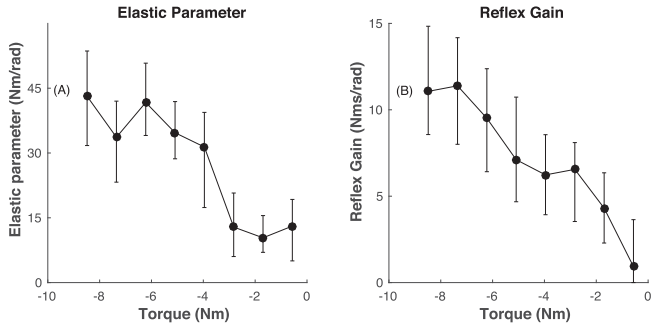

Fig. 10. Mean estimated intrinsic elastic parameter and gain of the reflex pathway bracketed by their 90% ranges using the SS-SDSS method as a function of ankle torque in the experimental study.

non-stationary data and studying systems with slow, time-varying behavior.

V. Discussion

A. Summary

This paper presented the SS-SDSS method for identification of the ankle joint stiffness parallel-cascade structure from short, stationary data segments. The method estimates an impulse response function to describe the intrinsic stiffness pathway, Tchebychev polynomials for the static nonlinearity of the reflex pathway and a state-space model for its linear dynamics. It also estimates the initial conditions for each segment. Simulation studies delineate the range of conditions for which the method can be expected to work successfully. Analysis of a pilot experimental data set demonstrates that the method works well in practice.

B. Initial Conditions

ICs are often ignored in constructing mathematical models for stable biological systems. This is a reasonable assumption when the data length is much longer than the system transient response as the contribution of ICs converges to zero. However, we hypothesized that ICs become significant in output prediction and parameter estimation for short data segments where the length of each data segment is comparable to that of the transient response due to ICs. SS-SDSS that is an extension of the SDSS method, enabled us to test this hypothesis. The main difference between the two methods is in accounting and identification of ICs. Consequently, we attributed the differences between the methods to the significance of accounting for the ICs.

It was demonstrated that accounting for the ICs increases the performance of the method in prediction of the output in both simulation (Fig. 7) and experimental (Fig. 9) studies. Furthermore, accounting for the ICs was also significant in reducing the inaccuracies associated with the estimation of the system parameters as evident in Fig. 8.

C. Simulation and Experimental Results

We verified the effectiveness of the SS-SDSS method in simulation studies mimicking realistic experimental conditions. The input signals were records of ankle joint angular position measured experimentally when position perturbations were delivered to subjects. This accounted for changes observed between the ideal position command and the delivered position due to the nonlinear filtering of the actuator and load. Similarly, the noise signals were records of joint torque measured when no position perturbations were delivered to the ankle. Thus, the simulations accounted for the non-Gaussian, non-white characteristics of experimental noise.

Simulations examined the range of parameters observed in real experiments. We explored different levels of the noise power and relative contribution of the intrinsic and reflex pathways, as these system factors are expected to affect the accuracy and precision of the decomposition and identification algorithm. The method's performance also depend on data factors: the number of data segments and their lengths. So, we examined different combinations of these up to the algorithm's limit. Fig. 4 documents the minimum number of segments and their lengths required for successful identification at a range of parameters mimicking different experimental conditions.

Simulation studies firstly demonstrate that the new method successfully decomposed the measured torque to the intrinsic and reflex torques. Secondly, they provide guidelines for the design of experiments, so the modeller would know how many segments to acquire prior to performing the experiment.

D. Application to Identification of Time-Varying Stiffness

Our limited simulation and experimental results for identification of slow, time-varying joint stiffness was used as proof-of-concept to show this application of the method. The non-stationary data were binned into short, quasi-stationary segments (based on the joint voluntary torque that was time-varying) and the method successfully recovered modulation of the important parameters of stiffness.

The experimental study demonstrated that both elastic parameter and reflex gain increased as a function of torque. This is consistent with previous studies and is presumably due to increase in the number of cross-bridges [33]. Increase in the reflex gain is inconsistent with previous stretch reflex studies in quasi-stationary conditions that showed the gain first increases and then decreases with voluntary torque [33]. This merits further investigation. Increase in the reflex gain can be due to increase in the excitability of the motorneuron pool

because of the descending drive or increase in sensitivity of the mechanoreceptors using the fusimotor mechanisms [37].

This utility of the SS-SDSS method can be compared to ensemble based [20] and Linear Parameter Varying (LPV) methods [22], [38], [39]. Ensemble based methods require many realizations with extremely repeatable time-varying behaviour [1]. SS-SDSS is not hinged upon these assumptions and works well as long as the non-stationary data can be binned to short, quasi-stationary data segments. It does not require equal-length segments and periodicity either. The LPV method requires a known scheduling variable that modulates the stiffness parameters. Identification of this scheduling variable requires *a priori* knowledge which is not always available [40] whereas SS-SDSS does not require a known scheduling variable. However, both ensemble and LPV methods are capable of identifying rapid changes in joint stiffness as is the case for example during walking [1] whereas the SS-SDSS method can only handle slow non-stationarities.

E. Algorithm Features

The SS-SDSS method is a MOESP-based subspace method and therefore inherits MOESP's attractive features. First, MOESP requires little *a priori* information while it is a parametric method as it estimates the order of the reflex linear system as part of the identification procedure; only an upper-bound on the system order must be specified *a priori*. This is important because while the reflex response is often assumed to be of second-order [33], it may be absent in some experimental conditions (e.g. plantarflexed positions) corresponding to a zero-order linear element or it can be of third-order in some conditions especially in pathological populations [41]. Thus, the true order of the system is not known to the modeller *a priori* and if selected incorrectly, will bias the measurement of stiffness. Second, it performs well with arbitrarily colored output noise; this is important because the color of the voluntary torque (considered as the output noise) is not generally known to the modeller. Third, it can be extended to identification from closed-loop data [42]. This is of particular importance when the joint interacts with a compliant load as it does in most functionally important tasks (e.g. control of body weight in upright stance) [43], [44].

The SS-SDSS method can be compared to others for identification of the joint biomechanics from short data segments. Ludvig and Perreault developed a nonparametric method for the identification of intrinsic joint stiffness [45]. It successfully identified stiffness of the knee during dynamic isometric muscle activation. Since it does not account for initial conditions, it is applicable to data where the segment length is larger than the system's time constant, e.g. intrinsic stiffness that has very fast dynamics. Zhao and Kearney [46] proposed a subspace approach to identify a general MIMO linear system encompassing the PC structure that accounted for initial conditions. However, it required all data segments to have equal lengths which is difficult to achieve due to the highly unpredictable nature of the system in real experiments. Moreover, it was not straightforward to relate the parameters of the MISO state-space model to the original stiffness parameters making it difficult to relate changes in the reflex pathway to the underlying static nonlinearity and linear dynamics. Kukreja *et al.* [47] identified a Hammerstein structure (applicable to the reflex stiffness path only) from short segments of data using a transfer-function identification technique. They considered and estimated initial conditions but their method performed poorly with colored noise [48]. Consequently, we believe that the algorithmic features of SS-SDSS makes it an attractive tool for measurement of joint stiffness from short data segments.

A potential limitation of the SS-SDSS as with all other subspace methods is that any delay in the reflex pathway must be known *a priori*. While the delay is almost invariant (typically 30-40ms) in healthy, adult humans, it might change in patients with neurological disorders. Fortunately, the delay can be easily identified using a cross-correlation analysis of position and EMG response. Alternatively, the value of delay can be found using a search to obtain the best fit.

F. Parallel-Cascade Structure

This method is designed to identify the parallel-cascade model structure for dynamic joint stiffness. This model structure is general and has been extensively used on the healthy and pathologic ankle, wrist, elbow, and trunk joints [12], [18], [28], [41]. In this model, the linear dependencies of input and output will be modelled by the IRF in the intrinsic pathway with a limited memory. The Hammerstein pathway models nonlinear aspects of the response, e.g. asymmetry in the rate sensitivity of the stretch reflex between flexor versus extensor muscles that has been reported in both upper and lower extremities [4], [27]. The nonlinear element of the Hammerstein model can be assigned a zero gain if there is no reflex component or become a linear model if the reflex response is linear.

Importantly, our method does not assume any *a priori* models for the elements of the parallel-cascade structure. Thus, we used a non-parametric impulse response function with unknown coefficients for the intrinsic dynamics. The main limitation of this model structure is that its length must be smaller than the reflex delay. The memory of the intrinsic dynamics is often less than 0.03 s with sampling frequency of 100 Hz as was the case in this study. However, the performance of the decomposition might degrade when the reflex delay becomes less than 0.03s which may be the case in the upper extremities with possibly lower reflex delays. Other types of structures have also been considered for the intrinsic dynamics in the literature such as impedance, admittance or compliance, in both time and frequency domains. There is, however, a direct mapping between the intrinsic stiffness dynamics that we considered and the other structures. Consequently, conversion to other model types is easy.

The assumed model structure for the reflex pathway is a Hammerstein structure that consists of a general static nonlinearity with unknown coefficients and a general, linear, dynamic element, with unknown order and dynamics. This structure is more general than a linear one as Hammerstein model encompasses linear systems. The Hammerstein structure might not

account for all the complex nonlinearities in reflex response and activation contraction dynamics of muscles. Nevertheless, we believe that the Hammerstein model provides a good first model since it can be regarded as the first element of a general parallel cascade expansion that can model any arbitrary nonlinear, dynamic system [49].

G. Other Applications

The SS-SDSS method would be a powerful tool to characterize joint stiffness in tasks where either only short segments of data can be recorded (e.g. high contraction levels) or when the underlying dynamics are slow time-varying (e.g. quiet stance). In future, it is of interest to explore this aspect of the algorithm.

An important clinical application of the method would be in distinguishing different types of hypertonia and assess the severity of impairment. The Ashworth test has been used extensively to assess hypertonia in patients with cerebral palsy, multiple sclerosis, spinal cord injury, stroke, etc [11], [50]. This test examines the resistance of the joint to passive movements in its range of motion by applying ramp and hold perturbation with different velocities. A trained physician manually applies the movement and scores the resistance based on the feeling of the resistance. It has been shown that this test is subjective and not reliable especially in lower extremities [51]–[53]. Our new method could be be a useful adjunct to quantify the neural and non-neural components of the tone in the joint's range of motion. Our experimental protocol is applicable by perturbing the joint with large ramp-and-hold movements with different velocities spanning the joint range of motion, superimposed on small PRALDS perturbations. SS-SDSS would then identify the dynamics after extracting short, quasi-stationary segments from the non-stationary data.

The method has applications to other systems showing time-varying or switching behaviour. For instance, the *Vestibulo Ocular Reflex* (VOR) circuit can be modelled with a Hammerstein structure; however, due to the switching nature of this type of eye movement, the VOR data consists of both slow and fast intervals sequentially. This results in variable length short segments of data in each mode with variable initial conditions. SS-SDSS method can be a useful tool for identification of such systems [30], [54].

REFERENCES

[1] H. Lee and N. Hogan, "Time-varying ankle mechanical impedance during human locomotion," *IEEE Trans. Neural Syst. Rehabil. Eng.*, vol. 23, no. 5, pp. 755–764, Sep. 2014.

[2] H. Lee, P. Ho, M. A. Rastgaar, H. I. Krebs, and N. Hogan, "Multivariable static ankle mechanical impedance with relaxed muscles," *J. Biomech.*, vol. 44, no. 10, pp. 1901–1908, Jul. 2011.

[3] W. Mugge, D. A. Abbink, A. C. Schouten, J. P. A. Dewald, and F. C. T. van der Helm, "A rigorous model of reflex function indicates that position and force feedback are flexibly tuned to position and force tasks," *Experim. Brain Res.*, vol. 200, no. 3, pp. 325–340, Jan. 2010.

[4] R. E. Kearney, R. B. Stein, and L. Parameswaran, "Identification of intrinsic and reflex contributions to human ankle stiffness dynamics," *IEEE Trans. Biomed. Eng.*, vol. 44, no. 6, pp. 493–504, Jun. 1997.

[5] M. Vlutters, T. A. Boonstra, A. C. Schouten, and H. van der Kooij, "Direct measurement of the intrinsic ankle stiffness during standing," *J. Biomech.*, vol. 48, no. 7, pp. 1258–1263, May 2015.

[6] Y.-S. Chen and S. Zhou, "Soleus H-reflex and its relation to static postural control," *Gait Posture*, vol. 33, no. 2, pp. 169–178, Feb. 2011.

[7] E. J. Rouse, R. D. Gregg, L. J. Hargrove, and J. W. Sensinger, "The difference between stiffness and quasi-stiffness in the context of biomechanical modeling," *IEEE Trans. Biomed. Eng.*, vol. 60, no. 2, pp. 562–568, Feb. 2013.

[8] A. L. Pando, H. Lee, W. B. Drake, N. Hogan, and S. K. Charles, "Position-dependent characterization of passive wrist stiffness," *IEEE Trans. Biomed. Eng.*, vol. 61, no. 8, pp. 2235–2244, Aug. 2014.

[9] E. M. Ficanha, G. A. Ribeiro, and M. Rastgaar, "Mechanical impedance of the non-loaded lower leg with relaxed muscles in the transverse plane," *Frontiers Bioeng. Biotechnol.*, vol. 3, p. 198, Dec. 2015.

[10] L. Bar-On, K. Desloovere, G. Molenaers, J. Harlaar, T. Kindt, and E. Aertbeliën, "Identification of the neural component of torque during manually-applied spasticity assessments in children with cerebral palsy," *Gait Posture*, vol. 40, no. 3, pp. 346–351, Jul. 2014.

[11] A. A. A. Alhusaini, J. Crosbie, R. B. Shepherd, C. M. Dean, and A. Scheinberg, "No change in calf muscle passive stiffness after botulinum toxin injection in children with cerebral palsy," *Develop. Med. Child Neurol.*, vol. 53, no. 6, pp. 553–558, Jun. 2011.

[12] C. Larivière, D. Ludvig, R. Kearney, H. Mecheri, J.-M. Caron, and R. Preuss, "Identification of intrinsic and reflexive contributions to low-back stiffness: Medium-term reliability and construct validity," *J. Biomech.*, vol. 48, no. 2, pp. 254–261, Jan. 2015.

[13] J. J. Palazzolo, M. Ferraro, H. I. Krebs, D. Lynch, B. T. Volpe, and N. Hogan, "Stochastic estimation of arm mechanical impedance during robotic stroke rehabilitation," *IEEE Trans. Neural Syst. Rehabil. Eng.*, vol. 15, no. 1, pp. 94–103, Mar. 2007.

[14] K. Jalaleddini, E. S. Tehrani, and R. Kearney, "A subspace approach to the structural decomposition and identification of ankle joint dynamic stiffness," *IEEE Trans. Biomed. Eng.*, to be published.

[15] K. M. Moorhouse and K. P. Granata, "Role of reflex dynamics in spinal stability: Intrinsic muscle stiffness alone is insufficient for stability," *J. Biomech.*, vol. 40, no. 5, pp. 1058–1065, 2007.

[16] E. J. Perreault, P. E. Crago, and R. F. Kirsch, "Estimation of intrinsic and reflex contributions to muscle dynamics: A modeling study," *IEEE Trans. Biomed. Eng.*, vol. 47, no. 11, pp. 1413–1421, Nov. 2000.

[17] K. M. Moorhouse and K. P. Granata, "Trunk stiffness and dynamics during active extension exertions," *J. Biomech.*, vol. 38, no. 10, pp. 2000–2007, Oct. 2005.

[18] R. Xia, A. Muthumani, Z.-H. Mao, and D. W. Powell, "Quantification of neural reflex and muscular intrinsic contributions to parkinsonian rigidity," *Experim. Brain Res.*, vol. 234, no. 12, pp. 3587–3595, Dec. 2016.

[19] R. F. Kirsch and R. E. Kearney, "Identification of time-varying stiffness dynamics of the human ankle joint during an imposed movement," *Experim. Brain Res.*, vol. 114, no. 1, pp. 71–85, Mar. 1997.

[20] D. Ludvig, T. S. Visser, H. Giesbrecht, and R. E. Kearney, "Identification of time-varying intrinsic and reflex joint stiffness," *IEEE Trans. Biomed. Eng.*, vol. 58, no. 6, pp. 1715–1723, Jun. 2011.

[21] E. J. Rouse, L. J. Hargrove, E. J. Perreault, and T. A. Kuiken, "Estimation of human ankle impedance during the stance phase of walking," *IEEE Trans. Neural Syst. Rehabil. Eng.*, vol. 22, no. 4, pp. 870–878, Jul. 2014.

[22] E. S. Tehrani, K. Jalaleddini, and R. E. Kearney, "Linear parameter varying identification of ankle joint intrinsic stiffness during imposed walking movements," in *Proc. 35th Annu. Int. Conf. IEEE Eng. Med. Biol. Soc. (EMBC)*, Jul. 2013, pp. 4923–4927.

[23] C. B. Lang and R. E. Kearney, "Modulation of ankle stiffness during postural sway," in *Proc. 36th Annu. Int. Conf. IEEE Eng. Med. Biol. Soc. (EMBC)*, Aug. 2014, pp. 4062–4065.

[24] L.-Q. Zhang and W. Z. Rymer, "Reflex and intrinsic changes induced by fatigue of human elbow extensor muscles," *J. Neurophysiol.*, vol. 86, no. 3, pp. 1086–1094, 2001.

[25] V. Z. Marmarelis, D. C. Shin, M. Orme, and R. Zhang, "Time-varying modeling of cerebral hemodynamics," *IEEE Trans. Biomed. Eng.*, vol. 61, no. 3, pp. 694–704, Mar. 2014.

[26] D. T. Westwick and E. J. Perreault, "Estimates of Acausal Joint impedance models," *IEEE Trans. Biomed. Eng.*, vol. 59, no. 10, pp. 2913–2921, Oct. 2012.

[27] D. G. Kamper and W. Z. Rymer, "Quantitative features of the stretch response of extrinsic finger muscles in hemiparetic stroke," *Muscle Nerve*, vol. 23, no. 6, pp. 954–961, Jun. 2000.

[28] L. Alibiglou, W. Z. Rymer, R. L. Harvey, and M. M. Mirbagheri, "The relation between ashworth scores and neuromechanical measurements of spasticity following stroke," *J. Neuroeng. Rehabil.*, vol. 5, no. 1, p. 18, 2008.

[29] A. A. Biewener, J. M. Wakeling, S. S. Lee, and A. S. Arnold, "Validation of hill-type muscle models in relation to neuromuscular recruitment and force–velocity properties: Predicting patterns of *in vivo* muscle force," *Integr. Comparative Biol.*, vol. 54, no. 6, pp. 1072–1083, 2014.
[30] A. Ghoreyshi and H. L. Galiana, "Simultaneous identification of oculomotor subsystems using a hybrid system approach: Introducing hybrid extended least squares," *IEEE Trans. Biomed. Eng.*, vol. 57, no. 5, pp. 1089–1098, May 2010.
[31] M. Verhaegen and V. Verdult, *Filtering and System Identification, A Least Squares Approach*. Cambridge, U.K.: Cambridge Univ. Press, 2007.
[32] K. Jalaleddini and R. E. Kearney, "Subspace identification of SISO hammerstein systems: Application to stretch reflex identification," *IEEE Trans. Biomed. Eng.*, vol. 60, no. 10, pp. 2725–2734, Oct. 2013.
[33] M. M. Mirbagheri, H. Barbeau, and R. E. Kearney, "Intrinsic and reflex contributions to human ankle stiffness: Variation with activation level and position," *Experim. Brain Res.*, vol. 135, no. 4, pp. 423–436, Dec. 2000.
[34] K. Mahata, J. Schoukens, and A. De Cock, "Design of Gaussian inputs for Wiener model identification," in *Proc. 17th IFAC Symp. Syst. Identificat. (SYSID)*, 2015, vol. 48. no. 28, pp. 614–619.
[35] M. Ranjbaran, K. Jalaleddini, D. G. Lopez, R. E. Kearney, and H. L. Galiana, "Analysis and modeling of noise in biomedical systems," in *Proc. IEEE Eng. Med. Biol. Soc.*, Jul. 2013, pp. 997–1000.
[36] C. M. Laine, E. Martinez-Valdes, D. Falla, F. Mayer, and D. Farina, "Motor neuron pools of synergistic thigh muscles share most of their synaptic input," *J. Neurosci.*, vol. 35, no. 35, pp. 12207–12216, 2015.
[37] K. Jalaleddini *et al.*, "Neuromorphic meets neuromechanics, part II: The role of fusimotor drive," *J. Neural Eng.*, vol. 14, no. 2, p. 025002, 2017.
[38] D. L. Guarin and R. E. Kearney, "Identification of a time-varying, box-jenkins model of intrinsic joint compliance," *IEEE Trans. Neural Syst. Rehabil. Eng.*, to be published.
[39] M. A. Golkar, K. Jalaleddini, E. S. Tehrani, and R. E. Kearney, "Identification of time-varying dynamics of reflex EMG in the ankle plantarflexors during time-varying, isometric contractions," in *Proc. 37th Annu. Int. Conf. IEEE Eng. Med. Biol. Soc. (EMBC)*, Aug. 2015, pp. 6744–6747.
[40] D. Ludvig and E. J. Perreault, "Task-relevant adaptation of musculoskeletal impedance during posture and movement," in *Proc. Amer. Control Conf. (ACC)*, Jun. 2014, pp. 4784–4789.
[41] M. Mirbagheri, H. Barbeau, M. Ladouceur, and R. Kearney, "Intrinsic and reflex stiffness in normal and spastic, spinal cord injured subjects," *Experim. Brain Res.*, vol. 141, no. 4, pp. 446–459, Dec. 2001.
[42] C. T. Chou and M. Verhaegen, "Subspace algorithms for the identification of multivariable dynamic errors-in-variables models," *Automatica*, vol. 33, no. 10, pp. 1857–1869, Oct. 1997.
[43] E. de Vlugt, A. C. Schouten, and F. C. van der Helm, "Closed-loop multivariable system identification for the characterization of the dynamic arm compliance using continuous force disturbances: A model study," *J. Neurosci. Methods*, vol. 122, no. 2, pp. 123–140, Jan. 2003.
[44] D. T. Westwick and E. J. Perreault, "Closed-loop identification: Application to the estimation of limb impedance in a compliant environment," *IEEE Trans. Biomed. Eng.*, vol. 58, no. 3, pp. 521–530, Mar. 2011.
[45] D. Ludvig and E. J. Perreault, "System identification of physiological systems using short data segments," *IEEE Trans. Biomed. Eng.*, vol. 59, no. 12, pp. 3541–3549, Dec. 2012.
[46] Y. Zhao and R. E. Kearney, "System identification of biomedical systems from short transients using space methods," in *Proc. IEEE Eng. Med. Biol. Soc.*, Aug. 2008, pp. 295–298.
[47] S. L. Kukreja, R. E. Kearney, and H. L. Galiana, "A least-squares parameter estimation algorithm for switched Hammerstein systems with applications to the VOR," *IEEE Trans. Biomed. Eng.*, vol. 52, no. 3, pp. 431–444, Mar. 2005.
[48] M. Ranjbaran and H. L. Galiana, "Identification of the vestibulo-ocular reflex dynamics," in *Proc. 36th Annu. Int. Conf. IEEE Eng. Med. Biol. Soc. (EMBC)*, Aug. 2014, pp. 1485–1488.
[49] M. J. Korenberg, "Parallel cascade identification and kernel estimation for nonlinear systems," *Ann. Biomed. Eng.*, vol. 19, no. 4, pp. 429–455, Jul. 1991.
[50] M. Blackburn, P. van Vliet, and S. P. Mockett, "Reliability of measurements obtained with the modified ashworth scale in the lower extremities of people with stroke," *Phys. Therapy*, vol. 82, no. 1, pp. 25–34, 2002.
[51] M. M. Mirbagheri, K. Settle, R. Harvey, and W. Z. Rymer, "Neuromuscular abnormalities associated with spasticity of upper extremity muscles in hemiparetic stroke," *J. Neurophysiol.*, vol. 98, no. 2, pp. 629–637, 2007.
[52] E. de Vlugt, J. H. de Groot, K. E. Schenkeveld, J. H. Arendzen, F. C. T. van der Helm, and C. G. M. Meskers, "The relation between neuromechanical parameters and ashworth score in stroke patients," *J. NeuroEng. Rehabil.*, vol. 7, no. 1, p. 35, 2010.
[53] C. G. M. Meskers, J. H. de Groot, E. de Vlugt, and A. C. Schouten, "Neurocontrol of movement: System identification approach for clinical benefit," *Frontiers Integr. Neurosci.*, vol. 9, p. 48, Sep. 2015.
[54] M. Ranjbaran, A. Katsarkas, and H. L. Galiana, "Vestibular compensation in unilateral patients often causes both gain and time constant asymmetries in the VOR," *Frontiers Comput. Neurosci.*, vol. 10, p. 26, Mar. 2016.

Kian Jalaleddini (S'08–M'16) received the B.Sc. degree in electrical engineering from the University of Tehran, Tehran, Iran, in 2007, the M.A.Sc. degree in electrical and computer engineering from Concordia University, Montréal, Canada, in 2009, and the Ph.D. degree in biomedical engineering from McGill University, Montréal, in 2015. He is currently a Post-Doctoral Scholar with the Division of Biokinesiology and Physical Therapy, University of Southern California. His research interests include analysis of biomedical signals and systems, development and application of system identification tools, exploring biomechanics of human joints, and spinal reflexes. He is a member of the IEEE Engineering in Medicine and Biology and Control System Societies. He has served as the Chair of the IEEE Engineering in Medicine and Biology Chapter, Montréal Section from 2011 to 2015 and a Secretary of the IEEE Montréal Section from 2010 to 2013.

Mahsa A. Golkar (S'13) received the B.Sc. degree in electrical engineering from the University of Tehran, Tehran, Iran, in 2007, the M.A.Sc. degree in electrical engineering from Concordia University, Montréal, Canada, in 2010, and the M.A.Sc. degree in biomedical engineering and image processing from the École Polytechnique de Montréal, Montréal, in 2013. She is currently pursuing the Ph.D. degree in biomedical engineering from McGill University, Montréal. Her research interests include analysis, modeling and identification of biomedical systems, development of system identification tools, and exploring the EMG-Torque dynamics.

Robert E. Kearney (M'76–SM'92–F'01–LF'13) received the bachelor's, master's, and Ph.D. degrees in mechanical engineering from McGill University in 1968, 1971, and 1976, respectively. He is currently a Professor and the Chair of the Department of Biomedical Engineering, Faculty of Medicine, McGill University. He maintains an active research program that focuses on using quantitative engineering techniques to address important biomedical problems. Specific areas of research include the development of algorithms and tools for biomedical system identification, the application of system identification to understand the role played by peripheral mechanisms in the control of posture and movement, and the development of signal processing and machine learning methods for respiratory monitoring. His research is supported by NSERC, CIHR, and the Qatar National Research Fund. He is a Professional Engineer and a fellow of the Engineering Institute of Canada and the American Institute of Medical and Biological Engineering.